*J. Fluid Mech.* (1991), *vol.* 223, *pp.* 241–252
*Printed in Great Britain*



# Examination of $v$-velocity fluctuations in a turbulent channel flow in the context of sediment transport

By T. WEI[1] AND W. W. WILLMARTH[2]

[1]Department of Mechanical and Aerospace Engineering, Rutgers University, Piscataway, NJ 08855, USA

[2]Department of Aerospace Engineering, University of Michigan, Ann Arbor, MI 48109-2140, USA

(Received 18 August 1989 and in revised form 6 June 1990)

This paper is a report on the mechanism of turbulent momentum transport normal to the wall in a turbulent wall-bounded flow. The objective of this study is to examine the 'background' turbulent flow field as a first step toward understanding suspended sediment transport. Specifically, the hypothesis that fine grain particles can be kept in suspension through a net upward momentum flux in a turbulent boundary layer is examined. The net momentum flux can arise if the probability density distribution of the fluctuating $v$-signal is positively skewed; i.e. the positive $v$-fluctuations are predominantly of large amplitude and short duration while the negative $v$-fluctuations are of small amplitude and long duration. High-resolution, two-component laser-doppler anemometer measurements of the $v$-velocity component in a fully developed turbulent water channel flow were examined spanning a Reynolds number range of 3000 to 23000. Averages of these signals demonstrate that, for very small particles, there is net upward momentum flux in the range $y^+ > 30$, while there is a net downward momentum flux in the range $10 \leqslant y^+ \leqslant 30$. Preliminary results which categorize the normal velocity according to quadrants of motion are also included.

## 1. Introduction

This paper is written to address the role that a turbulent boundary layer can play in sediment transport in river beds. Specifically, it will be demonstrated that positive skewness in the $v$-velocity fluctuations results in a net upward momentum flux. This momentum transport plays a role in keeping sediment suspended above the river bed floor.

In the mid-1960s, Bagnold (1966) wrote a comprehensive work describing the transport of sediment along a river bed. He identified two additional transport processes, which he termed as 'bedload' transport and 'suspended' transport. Bedload transport is the dragging motion of solid material along the river bottom due to the wall shear stress. In addition to the tumbling of large particles along the river bed, Bagnold observed that much sediment is carried downstream in the form of a suspension, i.e. suspended transport. He further observed that the suspended sediment does not settle over time. This observation led to the hypothesis that there must be some sort of flow phenomenon which constantly lifts sediment up from the river bottom and 'throws' it into a suspended cloud.

There are numerous mechanisms by which sediment may be suspended in a river.

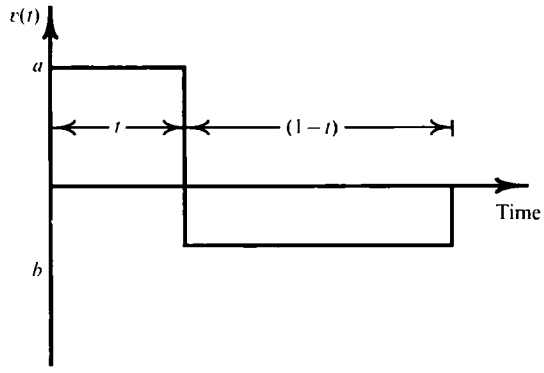


FIGURE 1. Simplified fluctuating $v$-velocity signal. The total duration of the signal has been normalized to unity.

One of the simplest, pointed out by one of the reviewers, results from random velocity fluctuations in a flow with a sediment concentration gradient. In this case, if the sediment concentration is highest close to the river bed floor, then an upward fluid motion will transport large amounts of sediment upward. A downward fluid motion will transport relatively fewer particles toward the bed because of the lower sediment concentration further away from the river bed. Consequently, random fluid motions normal to the river bed floor would result in a net upward transport of sediment in the presence of a sediment concentration gradient. It should be noted that this mixing will result in the elimination of the concentration gradient over time. Without another mechanism which maintains the concentration gradient, random fluctuations will no longer contribute to sediment suspension.

The importance of asymmetric $v$-probability densities in sediment transport was first observed by Bagnold (1966). He noted that the time average of the fluctuating $v$-signal must be zero. He pointed out that if the $v$-fluctuations were of equal amplitude and duration in both the positive and negative directions, there would be no net momentum flux acting on a suspended particle; on average, every suspended particle would drift back to the river bottom under the influence of gravity. He therefore argued that the flow close to the river bottom must be such that there are large-amplitude, short-duration, positive $v$-velocity fluctuations which push sediment away from the bottom. These upward thrusts would be opposed by long-duration, small-amplitude, negative $v$-fluctuations. In this scenario, suspended particles would drift down toward the river floor under the influence of gravity and the small-amplitude negative $v$-fluctuations. However, before the particles could settle on the bottom, they would be violently thrust upward, back into the flow.

Positive skewness of the fluctuating $v$-signal can be shown to result in a net upward momentum flux. Consider the simplified $v$-signal for flow over a flat plate shown in figure 1. This signal contains a single upward fluctuation of amplitude $a$, and duration $t$, and a single downward fluctuation with amplitude $b$, and duration $(1-t)$; the total duration of the signal is assumed to be unity. In order for the flow to remain parallel to the plate:

$$at + b(1-t) = 0. \tag{1}$$

Solving for $b$ in terms of $a$ and $t$ yields

$$b = \frac{at}{t-1}. \tag{2}$$

Next consider the momentum flux perpendicular to the wall. The momentum flux per unit mass in the positive $y$-direction is $a^2t$ and the momentum flux per unit mass associated with the downward $v$-fluctuation is $-b^2(1-t)$. Thus, perpendicular to the plate,

$$\text{Net momentum flux per unit mass} = a^2t - b^2(1-t). \tag{3}$$

Substitution of (2) into (3) yields

$$\text{Net momentum flux per unit mass} = a^2t(2t-1)/(t-1). \tag{4}$$

Note that the net momentum flux can be zero only when $t = 0$, $\frac{1}{2}$, and 1. If $t = 0$ or 1, then necessarily $a = b = 0$; the flow is laminar with no velocity fluctuations perpendicular to the wall. The case where $t = \frac{1}{2}$ implies that purely random $v$-velocity fluctuations will result in no net momentum flux. If $t \neq \frac{1}{2}$, the net momentum flux expression in (4) will be non-zero.

Bagnold's hypothesis, using the concept of skewed fluctuating $v$-signals, is consistent with experimental observations of turbulent boundary-layer flows with and without sediment particles. Kline *et al.* (1967) observed energetic upward ejections of low-momentum fluid in the near-wall region of turbulent boundary layers over a flat plate. They termed these upward motions 'bursts', and reported that most of the turbulent Reynolds stress was associated with these events. Grass (1971) conducted similar flow visualization studies for flow over rough walls. He observed that the presence of roughness elements changed the nature of the flow near the wall. However, fluid ejections and inrushes were still clearly discernable in rough-wall flows. Sumer & Oguz (1978) and Sumer & Deigaard (1981) conducted a series of experiments in which they tracked the trajectory of single and multiple particles in the near-wall region of smooth and rough walls. They observed that particles were in fact lifted from the wall and kept in suspension by the turbulent boundary-layer motions. They hypothesized that the particles were lifted by turbulent bursts and conjectured that the lifting of sediment from a river bottom also occurred during bursting.

One of the first attempts to quantify the net momentum flux in turbulent boundary layers was made by Leeder (1983). He used probability density distributions of the $v$-velocity component hot-film measurements of Brodkey, Wallace & Eckelmann (1974). Unfortunately, Leeder (1983) misinterpreted the density distributions; he assumed that $v$ had been non-dimensionalized by the mean centreline velocity when, in fact, $v$ was non-dimensionalized by the local mean velocity. Thus, while Leeder's (1983) conclusions are qualitatively consistent with the data of Brodkey *et al.* (1974), the quantitative analysis is errant.

Recently, Wei & Willmarth (1989) conducted a high-resolution, two-component laser-Doppler anemometry (LDA) study of a fully developed turbulent channel flow. The data of Wei & Willmarth (1989) have been re-examined to quantify the net upward momentum flux in a turbulent boundary layer flow due to asymmetric $v$-velocity fluctuations. The results presented in this paper represent an initial step in the quantification of suspended sediment transport in rivers. This is an examination of the baseline turbulent flow; it is recognized that a turbulent channel flow is hardly a river bed. The purpose of this paper is to show how the boundary layer on a smooth flat surface can contribute to the process of suspending sediment.

## 2. Definitions

In order to quantify the net momentum flux, it is necessary to distinguish when the $v$-velocity component is positive or negative; i.e. away from, or into the wall. Denote $v_{i+}$ as an instantaneous value of $v$, non-dimensionalized by the friction velocity, when $v$ is positive (flow away from the wall), and $v_{i-}$ as a dimensionless value of $v$ when the flow is toward the wall. The subscript $i$ represents the $i$th instantaneous data sample in the time-dependent data record. Further, define $T_+$ as the amount of time in a data record that $v$ is positive, and $T_-$ as the amount of time that $v$ is negative. Note that if the total duration of a data record is $T$, then

$$T = T_+ + T_-. \tag{5}$$

It is then possible to define the average value of the $v_{i+}$ and $v_{i-}$ as

$$\langle v_+ \rangle = \frac{1}{T_+} \sum v_{i+} \Delta t_i \tag{6}$$

and

$$\langle v_- \rangle = \frac{1}{T_-} \sum v_{i-} \Delta t_i, \tag{7}$$

respectively. Further, define the following averages:

$$\langle v_+^2 \rangle = \frac{1}{T_+} \sum [v_{i+}]^2 \Delta t_i \tag{8}$$

and

$$\langle v_-^2 \rangle = \frac{1}{T_-} \sum [v_{i-}]^2 \Delta t_i. \tag{9}$$

Equations (6) and (7) represent the mean upward and downward mass flux per unit area during the times $T_+$ and $T_-$, respectively. Similarly, (8) and (9) are related to the mean upward and downward momentum flux per unit area. In order to satisfy continuity (i.e. flow parallel to the wall):

$$\frac{1}{T}\{|\langle v_+ \rangle| T_+ - |\langle v_- \rangle| T_-\} = 0. \tag{10}$$

This is simply a rewritten version of (1). According to the physical arguments represented by (4) and Bagnold's suspended sediment transport hypothesis, if the fluctuating $v$-signal is positively skewed, then there should be a net upward momentum flux; $(T_+/T)\langle v_+^2 \rangle$ should be greater than $(T_-/T)\langle v_-^2 \rangle$. The net upward momentum flux would contribute to the lifting of sediment particles away from the river bottom.

## 3. Experimental method

A schematic diagram of the turbulent channel flow experiment developed by Wei & Willmarth (1989) appears in figure 2. The channel test section dimensions were 345.44 cm in length, 2.572 cm in width, and 30.48 cm in height. These dimensions correspond to the $x$-, $y$-, and $z$-directions, respectively. The measurement station was located 222.25 cm downstream of the test section inlet. An LDA measurement volume was created by the intersection of four laser beams as shown in figure 2. The beams were oriented so that two component measurements were made along the

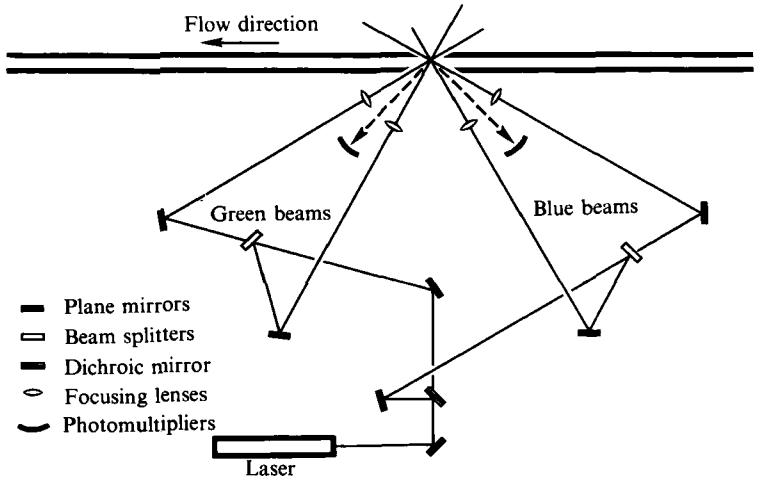


FIGURE 2. Top-view schematic drawing of the laser beam paths. Note that the beams angles/orientations are correct. However, the lengths are not to scale.

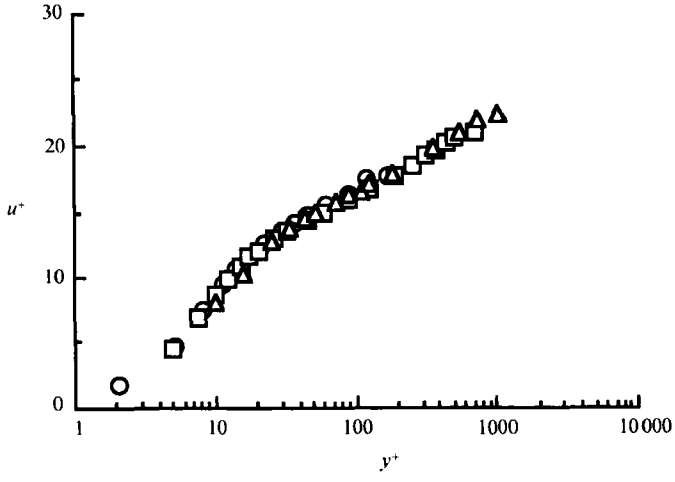


FIGURE 3. Mean velocity profiles, non-dimensionalized or inner variables, for the three Reynolds-number cases: ○, $Re = 2970$; □, $Re = 14914$; △, $Re = 22776$.

| $Re$ | $u_\tau$ (cm/s) | Viscous length $(\nu/u_\tau)$ (cm) | Probe dimension in viscous lengths |
|---|---|---|---|
| 2970 | 1.45 | 0.0076 | 0.66 |
| 14914 | 6.10 | 0.0018 | 2.76 |
| 22776 | 7.75 | 0.0013 | 3.94 |

TABLE 1. Significant flow parameters for the three Reynolds-number runs

principal axes of the flow, i.e. 45° into the wall and 45° away from the wall. Each laser beam was focused to a waist at the measurement volume, and the light scattered from the measurement volume was observed in sidescatter. In this manner, the spatial resolution of the LDA measurements was approximately 50 μm. The reader

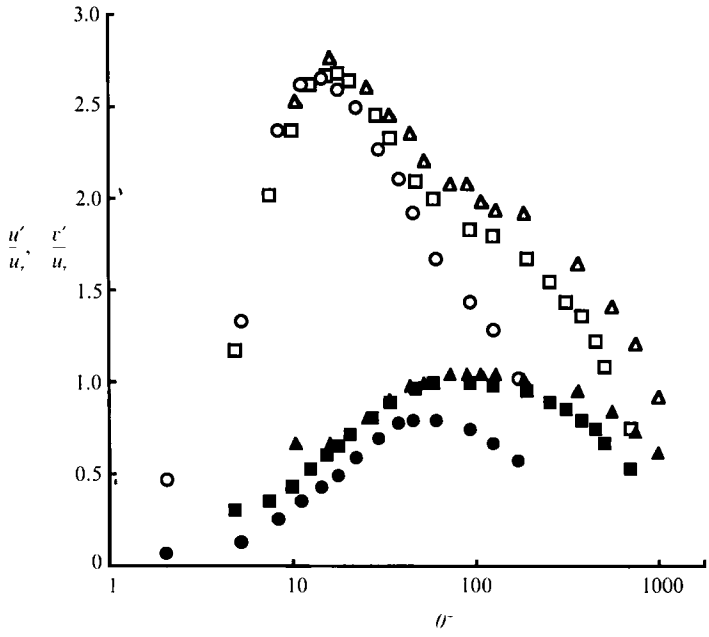


FIGURE 4. Streamwise and normal turbulence intensity profiles, non-dimensionalized with inner variables, for the three Reynolds-number flows: ○, $Re = 2970$; □, $Re = 14914$; △, $Re = 22776$. The open symbols represent the streamwise measurements, $u'$, and the solid symbols represent the component normal to the wall, $v'$.

is referred to Wei & Willmarth (1989) or Wei (1987) for specific details of the experiment.

Data from three runs in a Reynolds-number range of $2970 \leqslant Re \leqslant 22776$ are included in this report. Table 1 lists the significant flow parameters for each of the three cases. The Reynolds number is based on the centreline velocity, and half-channel width. Mean velocity profiles for the three runs are presented in figure 3, and turbulence intensity data appear in figure 4. For each of the three Reynolds-number runs, the LDA data rates were sufficiently high that it was possible to reconstruct the time-dependent $u$- and $v$-velocity signals (again, a detailed discussion may be found in Wei & Willmarth 1989). The $u$- and $v$-traces were reconstructed at even time intervals and digitally filtered with a Gaussian window. In this way, time averages could be obtained by simply ensemble averaging the reconstructed signals. Sufficiently long data records were obtained in order to assure accurate time averages.

## 4. Results and discussion

The difference in the magnitudes of $\langle v_+ \rangle$ and $\langle v_- \rangle$ are plotted in figure 5 as a function of distance from the wall for the three different Reynolds number runs. This demonstrates that there is an asymmetry in the fluctuating $v$-signal. Figure 6 is a plot of (10) for the three data sets non-dimensionalized with inner variables. In spite of the asymmetry, figure 6 clearly shows that continuity is satisfied; flow is parallel to the channel walls. Plots of

$$\text{Net non-dimensional momentum flux} = \frac{1}{T}\{\langle v_+^2 \rangle T_+ - \langle v_-^2 \rangle T_-\} \qquad (11)$$

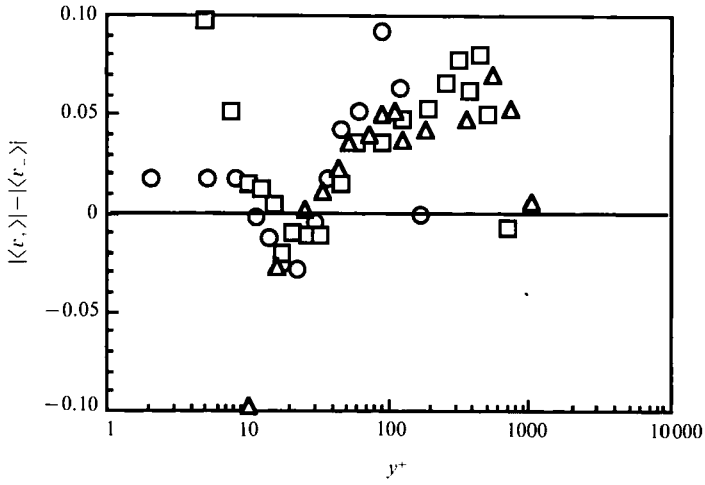


FIGURE 5. Profiles of $\{|\langle v_+\rangle|-|\langle v_-\rangle|\}$ for three Reynolds numbers (see (6) and (7) for the definitions of terms) non-dimensionalized with inner variables: ○, $Re = 2970$; □, $Re = 14914$; △, $Re = 22776$.

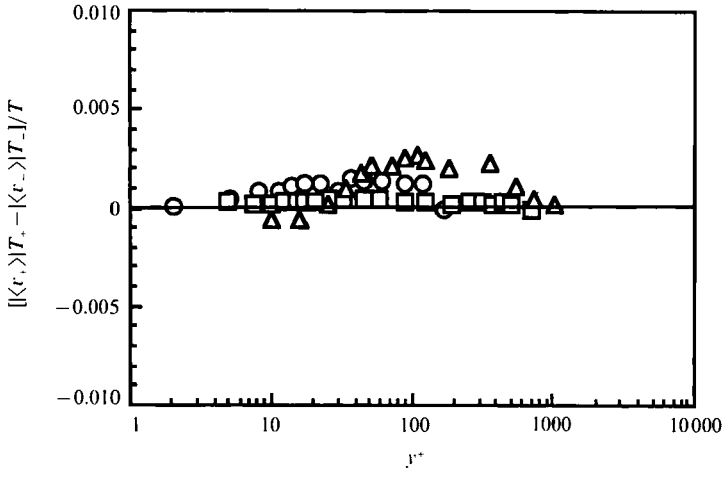


FIGURE 6. Plots of (10) for the three Reynolds numbers non-dimensionalized with inner variables. This plot demonstrates that the flow remains parallel to the channel walls. ○, $Re = 2970$; □, $Re = 14914$; △, $Re = 22776$.

appear in figure 7. Again, the data were non-dimensionalized by the density of water, the friction velocity and the kinematic viscosity. Figure 7 shows that there is a net upward momentum flux across most of the channel cross-section. This is consistent with the physical arguments of Bagnold (1966). However, in the range, $10 \leqslant y^+ \leqslant 30$, the reverse appears to be true. This was an unexpected result. It implies that there are large-amplitude, short-duration *negative* $v$-fluctuations in the turbulence production region which are offset by smaller-amplitude, longer duration *positive* $v$-fluctuations.

At the time of writing, a satisfactory explanation for this result has not yet been developed. Since comparing $\langle v_+\rangle$ with $\langle v_-\rangle$ is analogous to examining the skewness of $v$, it was not surprising to find that the skewness of $v$ was also negative in the range $10 \leqslant y^+ \leqslant 30$. The skewness data from Wei (1987) corresponding to the data used in

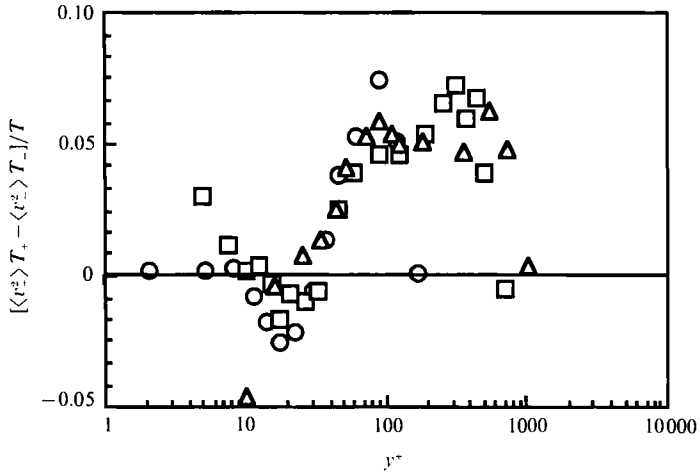


FIGURE 7. Profiles of $(1/T)$ $\{|\langle v_+^2\rangle| T_+ - |\langle v_-^2\rangle| T_-\}$, the net momentum flux, for the three Reynolds number non-dimensionalized with inner variables (see (8) and (9) for the definitions of terms). ○, $Re = 2970$; □, $Re = 14914$; △, $Re = 22776$.

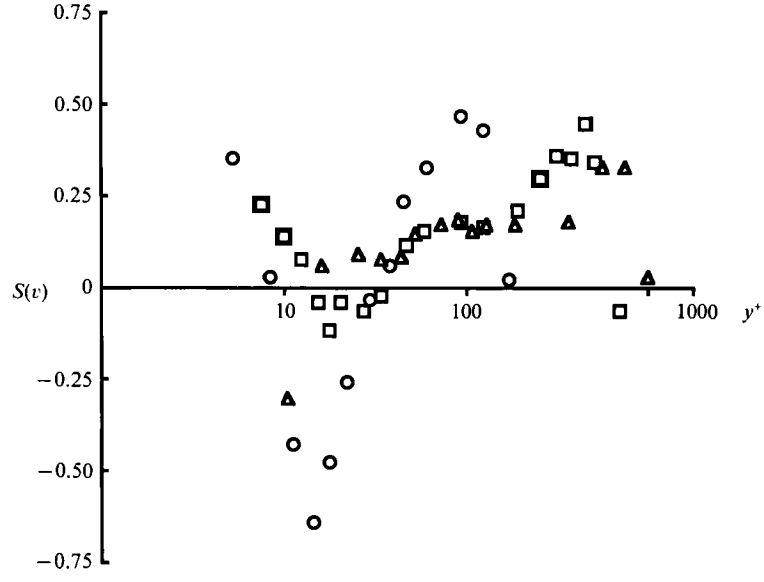


FIGURE 8. Profiles of the skewness in the fluctuating $v$-signals for the three Reynolds numbers (cf. Wei 1987): ○, $Re = 2970$; □, $Re = 14914$; △, $Re = 22776$.

this report are reproduced in figure 8. It can be seen from these $v$-skewness profiles that the skewness of the fluctuating $v$-signal is negative in the range $10 \leqslant y^+ \leqslant 30$. For $y^+ > 30$, the skewness values are positive. This is still an open research issue. A recent compilation of skewness data, reported by Klewicki & Falco (1988), shows a rough parity between the number of investigations which measured negative $v$-skewness values close to the wall and those investigations with positive $v$-skewness measurements.

For flow in a river, the issue of negative skewness in the near-wall region might not be of great practical importance. Actual geophysical flows are complex and three-

dimensional in nature. Examples of complexities include bends, rough walls, surface waves, convection, and multiphase flows, among many others. In addition, the Reynold numbers in a river are orders of magnitude larger than that found in the laboratory, and the turbulence lengthscales are extremely small. Grass (1971, 1983) and Jackson (1976) have examined the differences between geophysical boundary layers and the canonical boundary layers generally studied in the laboratory. Grass (1971) conducted hydrogen-bubble flow visualization experiments over a rough wall and found that large grain roughness elements enhanced the near-wall ejection process. Jackson (1976), in his literature review, noted that turbulent mixing has been reported to diminish with increasing suspended sediment concentrations. Both Grass (1983) and Jackson (1976) provide excellent qualitative descriptions of the sediment transport process. They both observed that the presence of suspended sediment and large wall roughnesses significantly alters the structure of the near-wall turbulence. It should therefore be noted that the results in this paper are for a rectangular channel flow and may differ from that of an actual river bed. For this experiment, however, the data show that there is a net upward momentum flux in the range of $y^+ \geqslant 30$.

The logical next step is to isolate which turbulent motions are principal contributors to the net upward momentum flux. The flow visualization studies of Kline *et al.* (1967), Grass (1971), Sumer & Oguz (1978), and Sumer & Deigaard (1981) indicate that upward momentum fluxes would be associated with the bursting process and the downward momentum fluxes would be caused by sweep motions. As a preliminary step towards this analysis, individual $v$-measurements were categorized and averaged according to the instantaneous quadrant of motion. That is, each instantaneous velocity measurement was categorized according to the sign of the $u$- and $v$-fluctuations. If both $u > 0$ and $v > 0$, the instantaneous measurement would be categorized as a Quadrant I motion. If $u < 0$ and $v > 0$, this was a Quadrant II motion, and so on. Turbulent bursts are primarily Quadrant II motions while sweeps are Quadrant IV motions. Time averages of $v$ and $v^2$ were computed for each of the four quadrants. The averaging time used was the total amount of time that $v$ was in the appropriate quadrant, $T_N$. Specifically, the average values of $v$ and $v^2$ associated with Quadrant $N$ (hereafter written as $\langle v_N \rangle$ and $\langle v_N^2 \rangle$, respectively) are

$$\langle v_N \rangle = \frac{1}{T_N} \sum v_{iN} \Delta t_i; \quad N = \text{I, II, III, IV} \tag{12}$$

and

$$\langle v_N^2 \rangle = \frac{1}{T_N} \sum v_{iN}^2 \Delta t_i; \quad N = \text{I, II, III, IV}, \tag{13}$$

where $v_{iN}$ and $v_{iN}^2$ are the instantaneous values of $v$ and $v^2$ when the corresponding velocity measurement is in Quadrant $N$. Again, continuity dictates that

$$\frac{1}{T}\{|\langle v_{\text{I}} \rangle| T_{\text{I}} + |\langle v_{\text{II}} \rangle| T_{\text{II}} - |\langle v_{\text{III}} \rangle| T_{\text{III}} - |\langle v_{\text{IV}} \rangle| T_{\text{IV}}\} = 0. \tag{14}$$

Note that $T$ is still the total duration of the data record. In this case

$$T = T_{\text{I}} + T_{\text{II}} + T_{\text{III}} + T_{\text{IV}}. \tag{15}$$

For each quadrant

$$\text{Mean momentum flux} = \frac{T_N}{T} \langle v_N^2 \rangle; \quad N = \text{I, II, III, IV}. \tag{16}$$

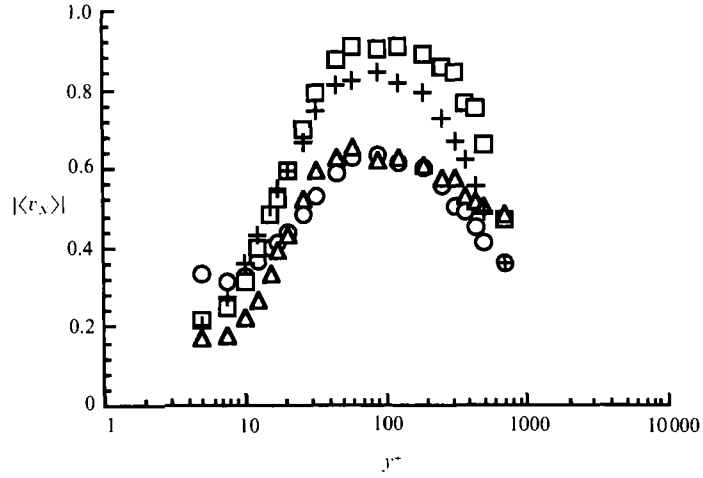


FIGURE 9. Average values of $|\langle v_N \rangle|$ in each of the four quadrants, non-dimensionalized with inner variables. Data in the figure were all taken from the $Re = 14914$ case. ○, $|\langle v_{\rm I} \rangle|$; □, $|\langle v_{\rm II} \rangle|$; △, $|\langle v_{\rm III} \rangle|$; +, $|\langle v_{\rm IV} \rangle|$.

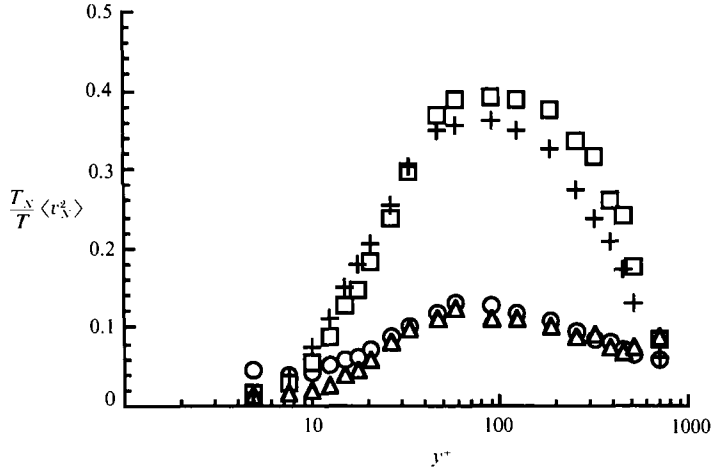


FIGURE 10. Average values of $(T_N/T)\langle v_N^2 \rangle$, the mean momentum flux in each of the four quadrants, non-dimensionalized on inner variables. Data in the figure were taken from the $Re = 14914$ case: ○, $(T_{\rm I}/T)|\langle v_{\rm I}^2 \rangle|$; □, $(T_{\rm II}/T)|\langle v_{\rm II}^2 \rangle|$; △, $(T_{\rm III}/T)|\langle v_{\rm III}^2 \rangle|$; +, $(T_{\rm IV}/T)|\langle v_{\rm IV}^2 \rangle|$.

Figure 9 shows the magnitudes of $\langle v_N \rangle$ for the $Re = 14914$ case non-dimensionalized with inner variables. Figure 10 shows the corresponding values of the mean momentum flux as defined in (16). The data in figure 10 were also non-dimensionalized with inner variables. The figures show that, for each $y$-location, the magnitudes of $\langle v_N \rangle$ and $\langle v_N^2 \rangle$ are larger in Quadrants II and IV than in Quadrants I and III. Further, the largest values of $|\langle v_N \rangle|$ and $\langle v_N^2 \rangle$ are found in Quadrant II for any $y$-location. Similar results were found for the $Re = 2970$ and 22776 data.

Quadrant II motions are associated with the bursting phenomenon, the sudden and violent upward ejections of low-speed, near-wall fluid away from the wall. It would be expected that the magnitudes of $\langle v_{\rm II} \rangle$ and $\langle v_{\rm II}^2 \rangle$ should be larger than in the other three quadrants for any given $y$-location. On the other hand, Quadrant IV motions are associated with the inrush of high-speed fluid toward the wall, the sweep.

In the sweep, the angle between the local instantaneous flow velocity vector and the wall is relatively small. Therefore, the magnitudes of $\langle v_{IV} \rangle$ and $\langle v_{IV}^2 \rangle$ should be less than the corresponding values in Quadrant II. There are no significant coherent structures associated with Quadrants I and III, the flow of high-speed fluid away from the wall and low-speed fluid toward the wall, respectively. This would explain why the magnitudes of $\langle v_N \rangle$ and $\langle v_N^2 \rangle$ in Quadrants I and III are less than in Quadrants II and IV.

At the time of writing, however, no distinction can be made between dynamically significant turbulent motions and those motions that do not contribute to turbulence production. Every instantaneous velocity measurement was included in the averaging process regardless of the dynamic importance. This means that there are a large number of measurements included in the averages in which there are no dynamically important events taking place. It is therefore at present impossible to determine the effect of the turbulent bursts (for example) on the suspended transport of sediment. The results of this investigation, however, clearly demonstrate that non-zero skewness in the $v$-probability density distributions leads to a net momentum flux. The direction of the momentum flux will depend on the sign of the skewness; positive skewness results in a net upward momentum flux. It is believed that there is a net upward momentum flux which is a contributing mechanism to the transport of sediment in river beds. Finally, there appears to be some ambiguity in the region $10 \leqslant y^+ \leqslant 30$; the present results show a negative $v$-skewness, implying a net downward momentum flux.

We wish to gratefully acknowledge the help of Professor F. K. Browand of the University of Southern California for suggesting the problem to us, and for his advice and comments on the work. We also acknowledge the assistance of Mr E. Kline of Rutgers University for generating the figures. The support through the Office of Naval Research by Dr M. M. Reischman is greatly appreciated.

## REFERENCES

BAGNOLD, R. A. 1966 An approach to the sediment transport problem from general physics. *US Geological Survey Paper* 422-I.

BRODKEY, R. S., WALLACE, J. M. & ECKELMANN, H. 1974 Some properties of truncated turbulence signals in bounded shear flows. *J. Fluid Mech.* **63**, 209.

GRASS, A. J. 1971 Structural features of turbulent flow over smooth and rough boundaries. *J. Fluid Mech.* **50**, 233.

GRASS, A. J. 1983 The influence of boundary layer turbulence on the mechanics of sediment transport, *Euromech 156: Mechanics of Sediment Transport 1982*. Rotterdam: A. A. Balkema.

JACKSON, R. G. 1976 Sedimentological and fluid-dynamic implications of the turbulent bursting phenomenon in geophysical flows. *J. Fluid Mech.* **77**, 531.

KLEWICKI, J. C. & FALCO, R. E. 1988 On accurately measuring statistics associated with small scale structure in turbulent boundary layers. *Mich. State Univ., Dept. of Mech. Engng Rep. TSL-88-4.*

KLINE, S. J., REYNOLDS, W. C., SCHRAUB, F. A. & RUNSTADLER, P. W. 1967 The structure of turbulent boundary layers. *J. Fluid Mech.* **30**, 741.

LEEDER, M. R. 1983 On the dynamics of sediment suspension by residual Reynolds stresses – confirmation of Bagnold's theory. *Sedimentology* **30**, 485.

SUMER, B. M. & DEIGAARD, R. 1981 Particle motions near the bottom in turbulent flow in an open channel. *J. Fluid Mech.* **109**, 311.

SUMER, B. M. & OGUZ, B. 1978 Particle motions near the bottom in turbulent flow in an open channel. *J. Fluid Mech.* **86**, 109.

WEI, T. 1987 Reynolds number effects on the small scale structure of a turbulent channel flow, Ph.D. thesis, The University of Michigan.

WEI, T. & WILLMARTH, W. W. 1989 Reynolds number effects on the structure of a turbulent channel flow. *J. Fluid Mech.* **204**, 57.